

Review papers

Recent developments, challenges, and future research directions in tomographic characterization of fractured aquifers

Lisa Maria Ringel^{a,*}, Walter A. Illman^b, Peter Bayer^a^a Applied Geology, Institute of Geosciences and Geography, Martin-Luther-University Halle-Wittenberg, Halle (Saale), Germany^b Department of Earth & Environmental Sciences, University of Waterloo, Waterloo, Ontario, Canada

ARTICLE INFO

This manuscript was handled by Corrado Corradini, Editor-in-Chief, with the assistance of Nick Engdahl, Associate Editor

Keywords:

Fractured geologic media
Hydraulic tomography
Pneumatic tomography
Inversion
Equivalent porous media
Discrete fracture network

ABSTRACT

This work reviews various studies of hydraulic and pneumatic tomography for estimation of flow properties of fractured geologic media with hydraulic and pneumatic tomography. The underlying conceptual inversion models can be broadly classified as continuum and discrete fracture network models and deterministic and stochastic approaches. A heterogeneous continuum method applies porous media parameters, while a DFN approach utilizes structural and hydraulic properties of fractures. An overview of field, laboratory, and synthetic studies with applications of hydraulic, pneumatic, or tracer tomography for the characterization of fractured geologic media shows that most studies rely on a heterogeneous continuum conceptual model and geostatistical methods to achieve a solution to the inverse problem. The application of a heterogeneous continuum model results in hydraulic properties that are representative of both fracture and matrix. Therefore, this approach may be more operationally useful for large scale sites with a non-negligible hydraulic conductivity of the rock matrix and high fracture intensity. The flow properties of single fractures can be estimated by applying a discrete fracture network (DFN) model. However, assumptions concerning fracture patterns and corresponding flow properties can lead to an oversimplified geological model. Possibilities for future research include integrating additional data and results from other inversion methods, the application of neural networks for inversion, the implementation of inversion results for the prediction and optimization of processes according to the planned application at the site, and opportunities for real-time inversion.

1. Introduction

Open fractures represent the preferential pathways for flow and transport in an otherwise intact rock matrix. They often form a network that results in a complex flow field depending on the size, geometry, and connectivity of fractures, and the hydraulic properties of the matrix. Despite the significant challenge to resolve these networks and to reliably describe their hydraulic properties, fractured sites are the target for various applications in hydrogeology and engineering. For instance, fractured aquifers host important groundwater resources (Chandra et al., 2019; Spencer et al., 2021; Wilske et al., 2020). Open fractures are also the main conduits for contaminant transport affecting groundwater resources (Berkowitz, 2002; Hadgu et al., 2017; Neuman, 2005). Extraction of geothermal energy or petroleum resources and sequestration of carbon dioxide rely on well-connected fracture networks by generating new fractures or by opening already existing ones through hydraulic, thermal, or chemical stimulation. Moreover, the properties

and the distribution of fractures are crucial for the evaluation of potential sites for nuclear waste repositories (Follin et al., 2014; Li et al., 2022), for the description of an excavation-induced damaged zone around tunnels and openings (Armand et al., 2014; de La Vaissière et al., 2015; Jalali et al., 2023), and for mining and extraction of minerals (Trabucchi et al., 2022). In all these different application areas, models and in particular specialized high-fidelity simulation tools are essential for improved understanding of subsurface processes. However, the applicability of these models depends on the reliability of fractured site characterization.

The fundamental issues and challenges regarding the characterization of fractured rocks for flow and transport quantification are discussed by Berkowitz (2002) and Neuman (2005). In contrast to studies reviewing monitoring and simulation methods for fractured sites (e.g., Berre et al., 2019; Lei et al., 2017; Viswanathan et al., 2022), this review focuses on the static characterization of the structural and hydraulic properties of fractured rocks with hydraulic and pneumatic tomography.

* Corresponding author.

E-mail address: lisa.ringel@geo.uni-halle.de (L.M. Ringel).

A general understanding of the structural properties of fractured rock sites, such as fracture intensities or prevalent fracture orientations, is derived by analyzing outcrops or evaluating the parameters of fractures intercepted by boreholes with borehole core samples or optical or acoustic televiewers (Armand et al., 2014; Barthélémy et al., 2009; Chandra et al., 2019; Follin et al., 2014; Ishibashi et al., 2016; Krietsch et al., 2018; Ma et al., 2022; Massiot et al., 2017; Pavičić et al., 2021; Ren et al., 2018; Vogler et al., 2018; Yin and Chen, 2020). The interpretation of single- and cross-borehole pumping/injection or tracer tests provides information about the hydraulic properties of the fracture network. The joint inversion of the recorded data from multiple tests is called hydraulic (HT), pneumatic (PT), or tracer (TT) tomography. These tomographic methods yield a two-dimensional (2D) or three-dimensional (3D) image of subsurface heterogeneity. Fractured rock sites typically pose a significant challenge for the application and evaluation of pumping/injection and tracer tests due to the sharp contrast between permeable fractures and the surrounding rock matrix.

Geophysical methods, such as stress-based tomography, electrical resistivity, seismic reflection, or ground penetrating radar offer only an indirect link between the hydraulic properties and the measured signal (Afshari Moein et al., 2018; Day-Lewis et al., 2017). A summary of various surface-based and borehole logging geophysical technologies suitable for the characterization of fractured media is provided by Day-Lewis et al. (2017). They also describe the measured parameters and indicate the potential target application of each method.

Cardiff and Barrash (2011) review studies utilizing HT and propose a procedure for the application of HT to the inversion of 3D unconfined permeable aquifers by conducting synthetic test cases. The characterization of fractured geologic media with a heterogeneous continuum conceptual model is reviewed by Illman (2014) discussing the benefits of HT over traditional characterization and modeling approaches. In our review, we discuss recent developments and challenges in fractured site characterization by HT and PT, such as the application of a discrete fracture network (DFN) model. For this purpose, we provide a theoretical overview of different conceptual models, inversion methods, and their application in practice in Section 2. In the subsequent section, we summarize studies concerning the characterization of fractured rock sites with HT, PT, and TT. This leads to a comparison between continuum and discrete conceptual models of fracture networks in Section 4. Finally, we discuss possible research directions in Section 5.

2. Overview of inversion methods applicable in fractured geologic media

2.1. Geometry of fracture networks

Fractures are mechanical discontinuities with a predominant direction, i.e., a void space confined on two sides by the surface of the intact rock. The length of a fracture can be variable ranging from centimeters to kilometers while the fracture aperture, i.e., the distance between fracture surfaces, is small compared to its length. The aperture of a fracture depends on the properties of the rock surfaces. Their fluctuations determine the local aperture distribution and are commonly described by statistical methods, such as a probability density function of the surface fluctuations, an autocorrelation function describing the nature of each surface, and an intercorrelation function to relate the fluctuations of the upper and lower surface (Adler et al., 2013; Mourzenko et al., 2018; Vickers et al., 1992; Vogler et al., 2017).

The geometric properties of fracture networks are characterized by the fracture intensity, the network connectivity, and the spatial correlation of the properties of individual fractures, mainly the aperture, length, and orientation of fractures (Berkowitz, 2002). The parameters of the fracture network can be described by statistical distributions, such as the power law distribution (Bour and Davy, 1997; de Dreuzy et al., 2012; Hyman et al., 2019). Thereby, the term fracture network implies an impervious or low-permeable rock matrix, such as crystalline or

metamorphic rocks. In contrast, a fractured porous medium has a non-negligible matrix permeability allowing for fluid exchange between fractures and the adjoining matrix (Adler et al., 2013; Berkowitz, 2002; Berre et al., 2019).

2.2. Experimental setup for pumping/injection or tracer tests

The pumping/injection or tracer tests that we are studying have a common principle. They repeatedly perturb the system under investigation by pumping or injecting some fluid or tracer into numerous borehole intervals (Fig. 1). To achieve this, various borehole intervals are isolated using packer systems, FLUTE liners, or grouting. Signals generated by this procedure are recorded at multiple monitoring intervals. The aim of these tests is to establish a relationship between the recorded signals and the connectivity or hydraulic properties of the flow paths between borehole intervals.

Single- and cross-borehole pumping/injection or tracer tests characterize the local hydraulic or pneumatic properties around a borehole interval (Brixel et al., 2020a; Guzman et al., 1996; Hsieh et al., 1983; Illman and Neuman, 2000; Ren et al., 2018), or the hydraulic or pneumatic properties of the connection between several intervals (Brixel et al., 2020b; Chuang et al., 2017; de La Vaissière et al., 2015; Hsieh et al., 1985; Frampton and Cvetkovic, 2010; Illman and Neuman, 2001; Jalali et al., 2018; Le Borgne et al., 2006; Paillet, 1995; Paillet and Morin, 1997; Tiedeman et al., 2010), the velocity distribution (Kang et al., 2015), transport properties (Cvetkovic et al., 2010; Cvetkovic and Cheng, 2011; Kittilä et al., 2019), or the effects from hydraulic stimulation (Amann et al., 2018; Kittilä et al., 2020). Moreover, they are applied for constraining the hydraulic properties of simulation models (Cvetkovic et al., 2007; Follin et al., 2014; Li et al., 2022). Applied tracer injections include salt (Chuang et al., 2017; Doetsch et al., 2012; Giertzuch et al., 2021a; Giertzuch et al., 2021b; Jardani et al., 2013), reactive chemicals (Illman et al., 2010; Yeh and Zhu, 2007), dye or DNA-labeled tracers (Kittilä et al., 2019; Kittilä et al., 2020), or heat (de La Bernardie et al., 2018; Hermans et al., 2015; Klepikova et al., 2014; Somogyvári et al., 2016). The standard approach for characterizing the heterogeneity of fractured rocks involves estimating local hydraulic conductivities or permeabilities from single-hole tests and interpolating these values using kriging, stochastic simulations, and geostatistical inverse modeling (Blessent et al., 2011; Park et al., 2004; Vesselinov et al., 2001a, 2001b; Yeh et al., 1996). We refer to Illman (2014) for additional references on mapping heterogeneity by single-hole and single cross-hole data while the focus of this review is on the simultaneous interpretation of all recorded pressure, hydraulic head, or tracer responses. The joint inverse modeling of multiple cross-hole pumping/injection or tracer tests yields an estimate of the appearance and connectivity of fractures or of the distribution of the hydraulic properties of fracture networks depending on the choice of the conceptual model utilized in inverse modeling.

2.3. Conceptual models utilized in inverse modeling

Different conceptual models have been developed for the representation of properties of fracture networks in inversion models. In general, we distinguish between continuum and discrete descriptions, and between deterministic and stochastic models. The continuum models consist of homogeneous and heterogeneous approaches. All parameters necessary for the description of the system are summarized in a parameter vector. A schematic overview of the conceptual inversion models is given in Fig. 2 for a fictitious two-dimensional (2D) example.

A continuum approach utilizes porous media parameters which are the spatial distributions of hydraulic conductivity K [m s^{-1}], permeability k [m^2], or transmissivity T [$\text{m}^2 \text{s}^{-1}$]. In addition, specific storage S_s [m^{-1}], storativity S [$-$], or porosity ϕ [$-$] fields are estimated for transient problems. The ratio K/S_s is the diffusivity D [$\text{m}^2 \text{s}^{-1}$]. In this

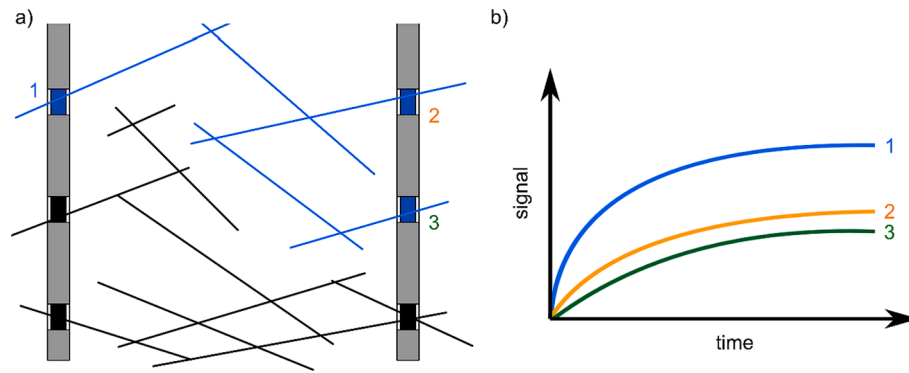


Fig. 1. 2D schematic experimental setup of pumping/injection or tracer tests (a). In this case, two boreholes and, in total, six injection and monitoring intervals are shown. Pumping in interval 1 causes responses in intervals 2 and 3 which are used in inverse modeling (b).

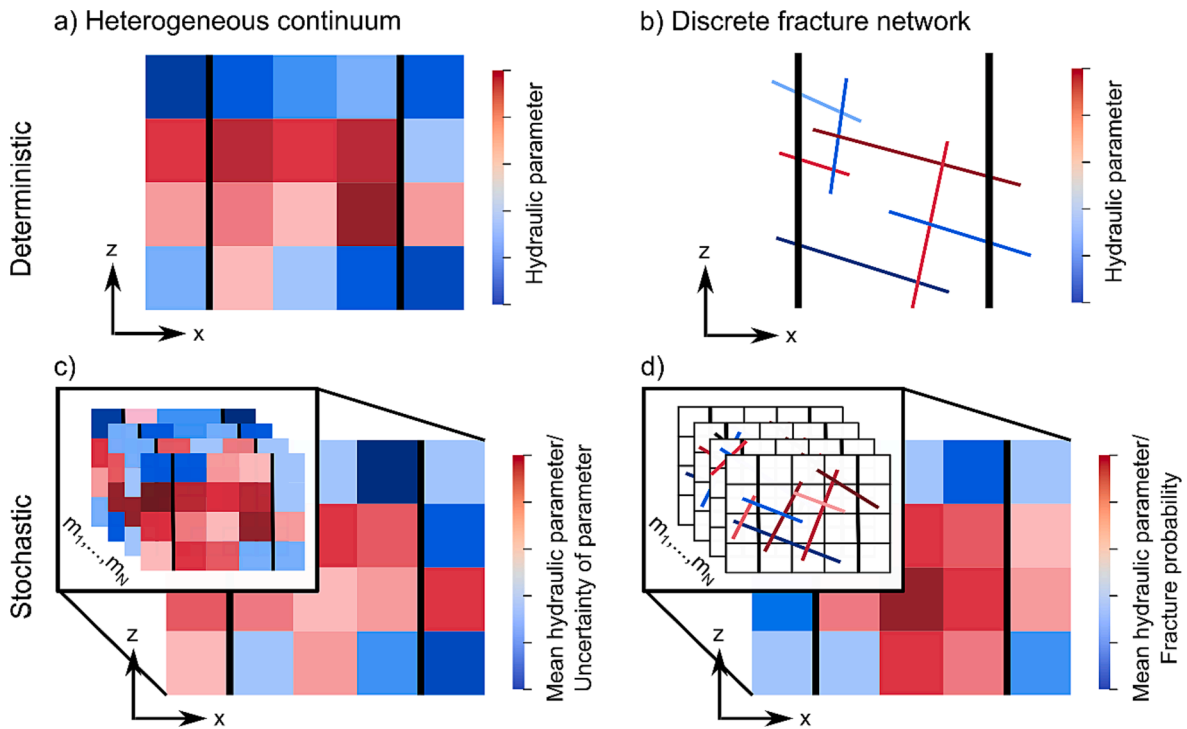


Fig. 2. Schematic overview of conceptual inversion models for a fictitious 2D example surrounding two boreholes (black lines) which are applied for the characterization of fractured geologic media, heterogeneous continuum (a and c) and DFN models (b and d) and deterministic (a and b) and stochastic (c and d) models. Hybrid models are a combination of heterogeneous continuum and DFN models. Different realizations of the parameter vector m_1, \dots, m_N which are generated by stochastic methods, are indicated in the boxes. The resolution of results depends on the scale of the investigated area and the element size.

study, we use bold symbols to indicate that these parameters are vectors with one value for each element. A homogeneous model is based on a spatial representative elementary volume (REV) which can be applied for dense and highly connected fracture networks (Berkowitz, 2002; Dong et al., 2019; Yeh et al., 2015). In this case, the hydraulic properties defined for a control volume (CV) can be applied independently of the spatial position of the CV (Yeh et al., 2015). In practice, the REV is often too large in comparison to the measurement intervals to be applicable and a heterogeneous continuum description is necessary (Neuman, 1987). Thereby, the hydraulic parameters are defined for small CVs without assuming a REV condition. The investigated area or volume is discretized into small porous media elements and the hydraulic parameters are estimated for each element (Dong et al., 2019; Zha et al., 2015), as illustrated in Fig. 2a and 2c. The size of the parameter vector equals the number of elements for steady-state HT or PT data or twice the number of elements for transient problems (Zha et al., 2015). In

order to assess the anisotropy of a system, each component of the hydraulic conductivity distribution can be treated as tensor to determine their directional and principal components. Since this approach introduces numerous additional unknowns, it is typically not utilized in inverse modeling for individual elements or grid blocks. Instead, it is more common to estimate the tensor components with a least-squares fit to various cross-hole flow tests on a REV scale by assuming a homogeneous anisotropic continuum (Hsieh et al., 1985; Neuman et al., 1984). The validity of the approach requires that the measured data fit the theoretical type curves and that the entries of the hydraulic conductivity tensor can be estimated reliably by minimizing a least-squares error.

A more direct representation of fractures and the anisotropy of the flow field is facilitated by applying a DFN model (Fig. 2b and 2d). Thereby, the fracture geometry is simplified to lower-dimensional objects that are 1D straight lines in 2D problems or 2D planes in 3D problems that are referred to as the so-called parallel plate model

(Zimmerman and Bodvarsson, 1996). The parameters that describe the fracture network are basically the number of fractures and, for each fracture, their structural (i.e., position, orientation, fracture shape, length, aperture) and hydraulic parameters as scalar quantities (hydraulic conductivity K_f , permeability k_f , or transmissivity T_f and specific storage $S_{s,f}$ or storativity S_f) as well as the distribution of each hydraulic parameter within one fracture. The cubic law relates the volumetric flow rate to the pressure or hydraulic head gradient by the hydraulic aperture a_f to the power of three. It holds for open fractures with negligible surface roughness (Berkowitz, 2002; Zimmerman and Bodvarsson, 1996). For the implementation in inversion models, the parameter vector of the DFN is reduced by applying assumptions and simplifications, e.g., about the fracture shape or orientation (Fischer et al., 2018c; Klepikova et al., 2013; Ringel et al., 2021). Therefore, the size of the parameter vector is the number of fractures times the number of parameters that are estimated for each fracture. Therefore, Fig. 2b and d vary according to the constant or variable DFN parameters specified for each study.

The hydraulic parameters of the rock matrix have to be incorporated in the inversion problem for sites consisting of fractured porous geologic media. This can be accomplished by hybrid models, which superimpose a DFN model and a heterogeneous continuum model by a conforming discretization at the boundaries between fracture and matrix or transfer terms to couple fracture and matrix elements. A specific type of hybrid model is the discrete fracture matrix model that includes large conductive fractures that are represented explicitly by their structural and hydraulic properties, while smaller, less conductive fractures are considered as hydraulic properties of the matrix (Berre et al., 2019). Multi-continuum models apply different continua for fracture and matrix. To date, these models have been applied only for the simulation of flow and transport in fractured rocks, not for inversion problems.

Inversion models are also categorized with deterministic and stochastic representations. A deterministic model applies a single parameter vector for describing the subsurface properties (Fig. 2a and 2b). The evaluated parameter vector is calibrated by minimizing an objective function which is the error between measured and simulated data in most studies (Klepikova et al., 2013). The uncertainty and non-uniqueness of the description of the properties of the fractured rock are considered by a stochastic approach that generates several realizations of the parameter vector. Thereby, the parameters are characterized by probability distributions and a mean parameter vector and its uncertainty or variance can be evaluated (Fig. 2c and 2d). An example of a stochastic heterogeneous continuum approach is the stochastic continuum method (SCM) introduced by Neuman (1987) and Tsang et al. (1996) for fractured geologic media.

2.4. Solution of the inverse problem

In general, forward or inverse problems provide a relation between experimental data and the parameters that are the quantity of interest to be estimated from experiments. Therefore, such problems comprise the following elements: the input data is obtained from observations or measurement campaigns, while the forward operator describes the present system that depends on a vector of model parameters (Aster et al., 2018). Depending on the problem, the forward operator is an ordinary or partial differential equation, or a system of equations. For most applications, the input data contains observation errors or measurement noise. The execution of the forward operator for a given parameter vector is a so-called forward problem, that is, the outcome of a tomography survey simulated based on model parameters. Thereby, conceptual model errors and discretization errors are introduced by assumptions applied to reduce the number of model parameters, simplifications of the underlying physics, or through the discretization of the differential equation in a numerical model.

In contrast to the forward problem, an inverse problem deals with

finding the model parameters given the input data (Aster et al., 2018). Several difficulties arise for the computation of inverse problems in practice. Due to measurement noise and errors or simplifications in the forward simulations an exact fit between the data simulated with a parameter set and the observed data is usually not possible. In addition, the number of parameters describing a system is often large making the solution nonunique. Therefore, assuming a simulation model with negligible errors, known and sufficient boundary and initial conditions, several model parameter realizations can lead to a minimum error between the simulated and observed data and therefore, give the best estimate of the hydraulic and structural parameters (Carrera et al., 2005; Yeh et al., 2015). A reduction of the number of parameters, e.g., due to the computational costs of iteratively solving the inversion problem, can lead to an oversimplification of the problem or may introduce structural errors (e.g., use of an inaccurate geological model or fracture distribution in a DFN). In that case, the solution can be less reliable and uncertainty estimates to be higher since it relies on improper physics or geometries despite a good fit of the simulated and observed data.

Depending on the input data, the conceptual inversion model, the forward model, and the scale of the investigated domain, different methods for the solution to the inverse problem with HT or PT data are feasible. The most common methods in hydrogeology are deterministic optimization approaches, geostatistical methods, and stochastic sampling methods. The different inversion methods for the characterization of fractured sites with HT, PT, and TT, the applied inversion method, and the results that are evaluated in each study are summarized in Table 1.

A deterministic solution is derived by minimizing the misfit between the measured data and the results from the forward simulation. The optimization is implemented generally as an iterative process of updating the parameter vector such that the observed head or pressure data matches the results of the forward simulation. The steps for solving an optimization problem are generally described in Carrera et al. (2005).

Travel time inversion is a specific type of inversion that applies a deterministic heterogeneous continuum model. The concept was adapted from seismic tomography to HT, PT, and TT. The basis is a relation between the travel time of the measured signal and the line integral of the reciprocal of the diffusivity (Brauchler et al., 2003). For advection-driven problems, such as heat transfer or tracer transport, the diffusivity can be replaced by the application of Darcy's law, i.e., porosity, permeability, and pressure gradient (Vasco and Datta-Gupta, 1999). For the inversion of HT data, the first derivative of the pressure or hydraulic head response is applied (Brauchler et al., 2013b). To distinguish preferential flow paths and to reduce the effects of diffusion, early-time diagnostics can be applied for thermal and hydraulic tomography (Somogyvári et al., 2016). The travel time is recorded at each receiver which functions as the input data for the solution of the inverse problem. The investigated domain is discretized and the trajectory length of the signal through each element is calculated, which depends on the material properties of each element. Then, the material parameters are adapted iteratively to match the observed travel times. The key advantages of the travel time approach are imaging of structural features representing high-diffusivity zones, requirement of less data for inverse modeling, and computational speed. However, the approach yields D tomograms and not K and S_s tomograms that are more useful for groundwater flow modeling.

A stochastic approach is based on the conditional probability of the parameter vector given the measured head or pressure signals. The sequential or the simultaneous successive linear estimator (SSLE or SimSLE) in Table 1 are frequently applied iterative geostatistical estimation methods that rely on the stochastic heterogeneous continuum representation of the subsurface properties. SSLE and SimSLE are an extension of kriging and cokriging methods (Xiang et al., 2009; Yeh and Liu, 2000). The element-wise natural logarithm of K and S_s are formulated as multi-Gaussian processes, i.e., the parameters are characterized by their mean, variance, and correlation among each other (Yeh et al.,

Table 1

Overview of studies (field, laboratory, or synthetic) concerning the characterization of fractured media with HT, PT, and TT, the inversion method, and corresponding results.

Site/Application	Study	Type of tomographic survey, data for inverse problem	Inversion method	Inversion results
Apache Leap Research Site (USA)	Vesselinov et al., (2001a,2001b)	Transient PT	Interpolation by pilot points; kriging	3D k and ϕ tomograms
Blair Wallis fractured rock hydrology research field (USA)	Ren et al. (2021)	Transient HT	SimSLE	2D K , S_s , and D tomograms
Göttingen (Germany)	Liu et al. (2022)	Thermal TT	Travel time	2D K tomogram
	Liu et al. (2023)	Tomographic slug tests	Travel time and attenuation-based inversion	3D K , S_s , and D tomograms
	Yang et al. (2020)	Transient HT	Travel time	2D D tomogram
Grimsel test site (Switzerland)	Kittilä et al. (2020)	Dye TT	Travel time	2D K tomogram before and after stimulation
	Klepikova et al. (2020)	Transient HT	Nelder-Mead optimization	T_r and S_r of 2D connectivity structure between injection intervals
	Meier et al. (2001)	Steady-state and transient HT	Geostatistical inversion	2D T tomogram
	Ringel et al. (2022)	Transient HT	MCMC	3D fracture probability and mean a_f
Meuse/Haute-Marne underground research lab (France)	Jalali et al. (2023)	Transient PT	Travel time and MCMC	3D D tomogram and 2D fracture probability
Mizunami underground research lab (Japan)	Illman et al. (2009)	Transient HT	SSLE	3D K and S_s tomograms
	Zha et al. (2015)	Transient HT	SimSLE	3D K and S_s tomograms
	Zha et al. (2016)	Transient HT	SimSLE	3D K and S_s tomograms
	Zha et al. (2017)	Transient HT	SimSLE	3D K and S_s tomograms
Ploemeur aquifer test site (France)	Dorn et al. (2013)	TT	Hierarchical rejection sampling (MC)	Connectivity and effective transmissivity of 3D fracture network
	Klepikova et al. (2014)	Flow tomography/ Thermal TT	Optimization	T_r of 2D connectivity structure between injection intervals
Salar de Atacama (Chile)	Trabucchi et al. (2022)	Transient drawdown data	Regularized pilot point stochastic inversion	2D K tomogram
Terrieu (France)	Fischer et al., (2017b)	Steady-state HT	Cellular automata-based deterministic inversion	2D T tomogram
	Fischer et al., (2018a)	Oscillatory HT	Interpretation of amplitude/ phase offset	Interpretation of the connection between boreholes as conduit, matrix, or hybrid
	Fischer et al., (2018b)	Oscillatory HT	Cellular automata-based deterministic inversion	2D T and S tomograms
	Fischer et al. (2020)	Steady-state HT	Discrete deterministic network inversion	T_r and 2D DFN structure; 2D T distribution of matrix
	Wang et al. (2016)	Steady-state HT	Sparse nonlinear optimization	2D T tomogram
	Wang et al. (2017)	Steady-state HT	Transition probability geostatistics and stochastic Newton MCMC	Stochastic EPM with three facies (karst, fracture, bedding); 2D T tomogram for each realization
Waiwera aquifer (New Zealand)	Somogyvári et al. (2019)	Borehole temperature profiles	MCMC	2D fracture probability
Former Naval Air Warfare Center (NAWC), West Trenton (USA)	Tiedeman and Barrash (2020)	Transient HT	Bayesian geostatistical approach	3D K tomogram
Xieqiao coal mine (China)	Wang et al. (2021)	Transient HT	SimSLE	2D K and S_s tomograms
Xindong coal mine (China)	Mao et al. (2018)	Transient HT	SimSLE	2D K and S_s tomograms
Laboratory studies	Brauchler et al. (2003)	Transient PT	Travel time	3D D tomogram
	Brauchler et al., (2013a)	Gas TT	Travel time	3D interstitial velocity tomogram
	Poduri et al. (2021)	Transient HT	Interpolation at pilot points by ordinary kriging	2D K and S_s tomograms
	Sharmeen et al. (2012)	Transient HT	SSLE	2D K and S_s tomograms
	Zhao et al. (2021)	Transient HT	SSLE	2D K and S_s tomograms

(continued on next page)

Table 1 (continued)

Site/Application	Study	Type of tomographic survey, data for inverse problem	Inversion method	Inversion results
Synthetic test cases	Chen et al. (2023)	Transient HT	Hierarchical parameterization, deep learning-based ensemble smoothing	2D fracture probability
	Cliffe et al. (2011)	Steady-state HT	Basis Vector Conditioning/ Bayesian Conditioning	T_r of 3D fractures
	Dodangeh et al. (2023)	Oscillatory HT and TT	Ensemble Kalman filtering	Test case 1: Fracture location and aperture Test case 2: Fracture density
	Dong et al. (2019)	Transient HT	SimSLE	2D K and S_S tomograms
	Fischer et al., (2017a)	Steady-state HT	Cellular automata-based deterministic inversion	2D T tomogram
	Fischer et al., (2018c)	Steady-state HT	Discrete deterministic network inversion	T_r and 2D DFN structure; 2D T distribution of matrix
	Hao et al. (2008)	Transient HT	SSLE	2D K and S_S tomograms
	Jiang et al. (2023)	Thermal TT and microseismicity events	MCMC	2D fracture probability
	Klepikova et al. (2013)	Drawdown and cross-borehole flow tomography	Quasi-Newton optimization	T_r of 2D connectivity structure between injection intervals
	Le Goc et al. (2010)	Steady-state HT	Hierarchical optimization	T_r of 2D flow channels
	Li et al. (2021)	Steady-state and transient HT	SimSLE	2D K and S_S tomograms
	Ma et al. (2020)	Transient production curves	Hierarchical parameterization, optimization, history matching	2D fracture probability
	Mohammadi and Illman (2019)	Steady-state and transient HT	SimSLE	2D K and S_S tomograms
	Ni and Yeh (2008)	Transient PT	SSLE	3D k and ϕ tomograms
	Redoloza et al. (2023)	TT	Genetic algorithm	Population of DFN models
	Ringel et al. (2019)	Transient HT/ TT	MCMC	2D fracture probability
	Ringel et al. (2021)	Transient HT	MCMC	3D fracture probability and mean a_r
	Somogyvári et al. (2017)	TT	MCMC	2D fracture probability
	Vu and Jardani (2022)	Steady-state HT	Convolutional neural networks	2D fracture geometry
	Vu and Jardani (2023)	Steady-state HT	Convolutional neural networks	2D fracture geometry and T tomogram of matrix
Wang et al. (2023)	Steady-state and transient HT	SimSLE	2D K and S_S tomograms	

1996; Zha et al., 2015; Zhu and Yeh, 2005). The estimate of the conditional mean parameter vector is updated iteratively according to the misfit between measured and simulated data weighted by a coefficient matrix. The coefficient matrix depends on the covariance and cross-covariance matrix and is calculated by a first-order approximation of the sensitivity of the simulated data to the current parameter estimate (Yeh et al., 1996). Additional head or pressure signals can be included either sequentially or simultaneously. The travel time inversion and the geostatistical inversion as implemented by SimSLE are compared by Qiu et al. (2023) for a heterogeneous synthetic test case. We refer to the respective references for further inversion algorithms, i.e., to Cardiff and Barrash (2011), Kitanidis (1995), and Tiedeman and Barrash (2020) for the quasilinear geostatistical algorithm, to Blessent et al. (2011), Park et al. (2004), and Wang et al. (2017) for the transition probability geostatistical method, and to Dorn et al. (2013), Ringel et al. (2021), and Somogyvári et al. (2017) for stochastic sampling methods, such as Monte Carlo (MC) or Markov chain Monte Carlo (MCMC) sampling. The parameter vector can be updated at specific time steps using techniques such as Kalman filtering (Dodangeh et al., 2023; Panzeri et al., 2013) or history matching (White, 2018) when new data is obtained.

3. Summary of tomography experiments and synthetic applications

The overview in Table 1 compares different inversion methods for

the characterization of fractured media with an emphasis on the obtained results. Table 1 demonstrates that most field studies rely on a heterogeneous continuum inversion model which allows the evaluation of distributions of porous media parameters as shown in Fig. 2a and 2c for a fictitious example in 2D and accordingly in 3D. The variance of the tomogram of estimated parameters can be analyzed additionally in the case of stochastic conceptual models which are the geostatistical algorithms.

The field studies summarized in Table 1 are grouped in Fig. 3 according to the scale and dimension of the investigated region and the type of conceptual inversion model. Fig. 3 shows that most studies applying a DFN model are smaller scale, while heterogeneous continuum methods are larger scale, from decimeters to kilometers. The tomograms of porous media parameters can be improved by the incorporation of specific prior knowledge (Poduri et al., 2021; Zha et al., 2017; Zhao et al., 2021) or through the analysis at high spatial resolution to distinguish between conduit and matrix elements in the tomogram (Fischer et al., 2017b; Fischer et al., 2018b). Further information about the fracture network can be gained by particle transport simulations to investigate fracture connectivity (Tiedeman and Barrash, 2020) or the comparison with forward simulations of synthetic test cases with similar properties as the site (Sharmeen et al., 2012; Zha et al., 2015).

The studies applying a deterministic DFN model (Fig. 2b) estimate less parameters of the fracture network than stochastic DFN models since the stochastic approach can consider the non-unique relation

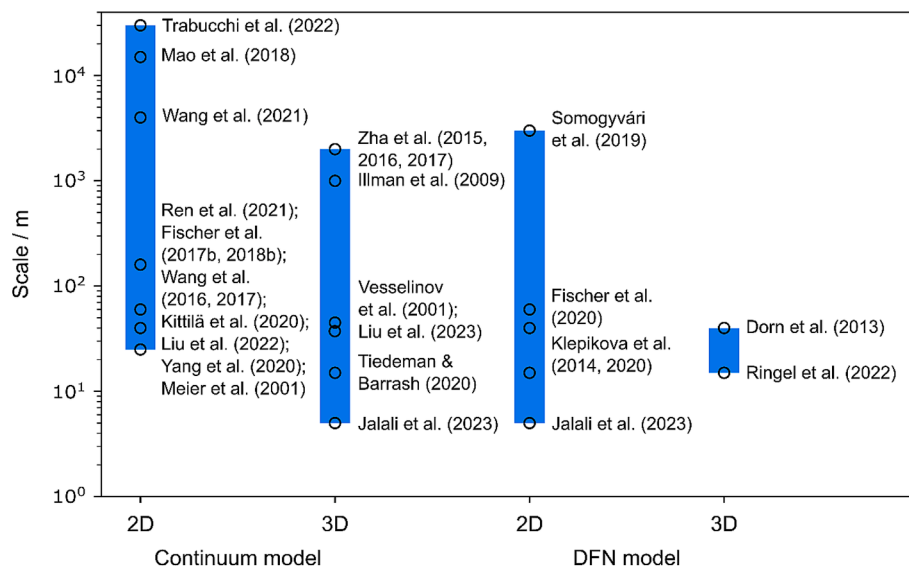


Fig. 3. Differentiation of field studies (Table 1) according to the conceptual inversion model, the dimension, and the scale of the investigated region. Here, scale refers to the maximum length of the evaluated tomogram of hydraulic or fracture parameters. The bars on the chart indicate the extent of the scale on which each conceptual model was used.

between head or pressure signals and the hydraulic and structural properties of the DFN model. Klepikova et al. (2014) and Klepikova et al. (2020) estimate transmissivity and storativity (Klepikova et al., 2020) of predefined structures that connect the injection and observation intervals. Fischer et al. (2020) partition the investigated area in subspaces and adjust the fracture properties in each subspace node-to-node according to six predefined structure possibilities. In a second step, the transmissivity of the fracture element is calibrated. Jalali et al. (2023), Ringel et al. (2022), and Somogyvári et al. (2019) utilize MCMC sampling to generate DFN realizations and estimate the number of fractures and position and length of each fracture which are evaluated as map of fracture probabilities (Fig. 2d). In these studies, the fracture shape is simplified and the possible fracture orientations are limited to two fracture sets according to borehole logs of fracture properties. In addition to the structural properties of fractures, Ringel et al. (2022) also adjust the hydraulic aperture of each fracture.

4. Comparison between DFN and continuum conceptual models

In the following, we compare continuum and DFN models and describe potential drawbacks and difficulties in the implementation of the respective conceptual model based on state-of-the-art inversion algorithms (Section 2.4) and the results of field, laboratory, and synthetic studies (Table 1).

Heterogeneous continuum models result in smooth images of hydraulic parameters due to being representative of the hydraulic properties of fracture and matrix. For this reason, the continuum representation provides good results for fractured rocks with a permeable matrix (Liu et al., 2022; Liu et al., 2023; Yang et al., 2020). Moreover, Dong et al. (2019) demonstrate for three synthetic test cases with an increasing fracture intensity that the accuracy of the K and S_S tomogram and the validation, which is the prediction of observed heads not used for the inversion, improves with an increased fracture intensity. The authors also show that the predicted response can be overestimated for receiver points not connected to the fracture network. Instead of differentiating between the influence of single fractures and between fractures and matrix, the specification of high and low conductive zones of the investigated volume is potentially more important, especially for large scale HT surveys. Therefore, continuum models have been preferred for characterizing sites ranging from hundreds of meters to kilometers in scale (Illman et al., 2009; Mao et al., 2018; Trabucchi

et al., 2022; Wang et al., 2021; Zha et al., 2015; Zha et al., 2016; Zha et al., 2017). DFN models, except for Somogyvári et al. (2019), are not applied at these scales, as shown in Fig. 3.

In contrast, the DFN conceptual model can delineate the strong heterogeneity of the K and S_S distribution caused by the appearance of a fracture network in rocks with a low-permeability matrix and on a small scale of the investigated site (Fig. 3). The major drawback of the DFN model is the definition of reasonable assumptions to reduce the number of parameters to be adjusted by the inversion. For example, assumptions regarding active and inactive fractures in terms of flow and transport may need to be made. For this reason, the resulting DFN models are like a projection of the real fracture network onto a lower-dimensional subspace. For instance, Fischer et al. (2020), Klepikova et al. (2020), Ringel et al. (2022), and Somogyvári et al. (2019) estimate constant hydraulic properties within a fracture segment and the fracture shape is simplified. Constraints regarding the DFN properties and especially a fixed DFN pattern can lead to a less accurate geological model which causes high errors when predicting independent validation results and in general unrealistic parameter estimates. This is a more important issue for deterministic DFN models since the number of parameters has to be reduced for deterministic approaches to avoid an underdetermined system of equations for the solution of the optimization problem. In addition, the setup of constraints and simplifications is also more challenging over a larger scale. The fracture transmissivity is assumed to depend on the hydraulic aperture according to the cubic law in Jalali et al. (2023), Ringel et al. (2022), and Somogyvári et al. (2019). The cubic law (Witherspoon et al., 1980) was derived by simplifying the Navier-Stokes equations for small Reynolds numbers, which implies viscous instead of inertial flow behavior, small changes of the velocity in the fracture plane, and no velocity component normal to the fracture plane (Zimmerman and Bodvarsson, 1996). Accordingly, the derived transmissivity does not consider a varying surface roughness and contact areas between the two surfaces even with a local cubic law assumption (Berkowitz, 2002). The reliance of the transmissivity on the hydraulic aperture can be avoided by estimating fracture conductivity and aperture independently. However, that increases the size of the parameter vector of the inversion problem by the hydraulic conductivity of each fracture segment.

The application of a DFN conceptual model for fractured porous media requires one to distinguish between the effects of fracture and matrix on flow. This can be achieved by either reasonable estimates for

Table 2
Overview of possible applications and drawbacks for continuum and DFN conceptual inversion models.

	Potential target applications	Difficulties
Heterogeneous continuum models	Large scale High fracture density	Smooth tomograms Hydraulic parameters representative of both fracture and matrix
DFN models	Fractured porous media Small scale	Simplifications concerning fracture shape and distributions of DFN parameters
	Low-permeability rock matrix Quantification of flow properties of single fractures	Reliability of cubic law for estimating fracture transmissivity

the initial values of the hydraulic conductivity of fracture and matrix or by suitable upper and lower limits on both conductivities (Fischer et al., 2020).

Overall, we conclude that the continuum representation is well suited where the influence of single fractures is small, which is the case for high fracture densities, large scales, and fractured porous media. The DFN model has advantages where the quantification of these effects is of interest. Therefore, we recommend the DFN conceptual model on a generally smaller scale and for a low-permeability rock matrix, such as crystalline rock. The comparison is summarized in Table 2 by potential target applications and difficulties of both conceptual models.

The computational costs of solving the inverse problem depend not directly on the choice between a continuum or a DFN approach, but on the implemented forward model and thereby, on the scale of the investigated domain, the simulation time, and the temporal and spatial discretization. Due to the explicit discretization of fractures in the DFN model, the computational costs of the DFN model increase with fracture density. The necessary number of forward simulations depends on the convergence properties of the applied inversion algorithm. Travel time inversion is an exception since this method is based on calculated travel times through ray tracing instead of forward simulations. Because of this, only the volume between boreholes can be characterized with the travel time inversion algorithm (Brauchler et al., 2003; Qiu et al., 2023).

5. Summary and research directions

The inversion of HT and PT data to obtain an image of the subsurface properties is an ongoing challenge with several possible directions for future research. Generally speaking, there is no best conceptual model that can handle all possible geologic applications and scales. However, the advantages of the DFN and continuum conceptual models can be combined, for example by locating potentially highly fractured zones according to the zones in the tomograms obtained from a heterogeneous continuum approach that indicate a high hydraulic conductivity or low specific storage. Then, the properties of these zones can be inferred with a DFN model to evaluate the fracture network further applying each conceptual model at the scale where it is more suitable. In addition, the hydraulic conductivity tomograms and the variance of the results as obtained from stochastic inversion algorithms can be applied directly as element-wise Gaussian prior distribution in the Bayesian equation or as a proposal function for MCMC algorithms. This offers us an opportunity for the joint inversion of discrete and continuum approaches.

The quantification of reliability and appropriate resolution of the inversion results are still open questions (Illman, 2014). A direct evaluation of the error or visual comparison between the inversion results and the reality is only possible for synthetic or laboratory test cases. For field studies, the reliability and implementation of the applied inversion method can be verified in general by developing the inversion algorithm

with several synthetic and laboratory test cases. The inversion results of a field site can be validated by simulating the outcome of hydraulic, pneumatic, or tracer tests that were not used for the solution of the inversion problem and by comparing predicted and measured draw-down, pressure change or tracer breakthrough data. However, the simulation of tracer breakthrough data requires additional parameters that are not estimated with HT or PT due to a different forward problem, such as heat capacity or thermal conductivity for heat tracer tests. In addition, the inversion results can be checked by comparison with other studies and data (Illman et al., 2009; Ringel et al., 2022; Trabucchi et al., 2022). Overall, the number of cross-hole pumping/injection tests, the scale of the site, the size of the elements in the tomogram, and the conceptual simplifications made in cases where a DFN model is applied can all impact the reliability of the inversion results. A challenge for future research is identifying the most useful additional information to maximize the reliability of the tomogram of hydraulic properties or the inferred DFN model, for example the best-suited complementary geophysical method. The ideal field data to complement the tomographic methods discussed here will depend on the prior information stage, the conceptual model of the tomographic inversion, and the scale of the site. For instance, a geologic model of the site, geophysical inversion results, or hydraulic parameter estimates from single-hole and cross-hole pumping tests can be applied as prior distributions for HT or PT inversion. Fracture properties as obtained by outcrops or optical or acoustic televiewer logs can support the definition of reasonable constraints on structural parameters of fractures. Flowmeter and/or groundwater temperature surveys can be conducted to identify active versus inactive fractures. In porous media aquifers, cross-hole flowmeter surveys have also shown to provide valuable information on connectivity to improve HT estimates (Luo et al., 2023). These additional studies can be used to confirm the general trend and the qualitative hydraulic properties, but not the exact values of hydraulic parameters or fracture probabilities. Moreover, for the DFN approach, the reliability depends mainly on the simplification on the DFN structure to reduce the number of unknown parameters.

The application of machine learning algorithms such as neural networks to HT is still in its early stages since machine learning has been demonstrated only for 2D synthetic test cases. Deep learning algorithms attempt to link hydraulic head measurements to fracture network patterns (Vu and Jardani, 2022) and/or hydraulic parameters (Guo et al., 2023; Vu and Jardani, 2023) through various neural network algorithms. The algorithms require a large training dataset to handle datasets not covered during the learning phase. For example, Vu and Jardani (2022, 2023) utilized neural networks to map a simple 2D fracture network embedded in a heterogeneous aquifer through the inversion of hydraulic head data obtained from a HT survey. In this synthetic study, the authors demonstrated the potential for neural networks to map the fracture network, but these studies rely on a dense network of observation wells which might not be available for many settings in practice. Moreover, the accuracy of the approach depends heavily on the dataset utilized during the training of the neural network, and the quality of the results is still an open question, especially in practice with simplifications in the conceptual model or potentially insufficient boundary and initial conditions applied for the forward simulations. Further work is needed to make meaningful comparisons against existing inversion approaches and to evaluate if machine learning and traditional approaches could be combined.

An important direction for future research is the applicability of the inversion results to simulate and predict groundwater flow or concentration data independent of the pumping or tracer tests used for the inversion and, in a next step, also to conduct coupled thermal-hydraulic-chemical-mechanical (THMC) process simulations. For instance, hydromechanical (HM) simulations use DFNs generated according to analogue or borehole mapping, statistical data, such as fracture length, orientation, and location distributions, or geomechanical DFNs (Lei et al., 2017), but no DFNs or tomograms of hydraulic properties inferred

with HT or PT data are applied. Similar to the validation of HT or PT inversion results with tracer tests, not all parameters necessary for these simulations can be estimated with HT or PT. Because of the different forward simulation problem, one has to rely on additional values from the literature or conduct further studies. The precision of simulations or predictions based on inversion results is highly dependent on the quality of the inversion results as described in the previous paragraph. Furthermore, the accuracy of supplementary values that are not estimated by HT or PT inversion must also be considered. By employing stochastic conceptual models and by carrying out simulations with different realizations of the parameter vector, we can obtain an estimate of the uncertainty of the prediction. Another point is selecting the appropriate conceptual inversion model based on the scope of the simulation. When the contribution of the rock matrix cannot be ignored, as in situations involving matrix diffusion, sorption, or thermal conduction, a continuum model is favorable (Hadgu et al., 2017). The opening of fractures and the increase of the fracture aperture as relevant for geothermal applications can be modeled more directly by the DFN conceptual model. A next step is linking the static characterization with HT or PT and the dynamic modeling and monitoring during the operation. This allows for an update of the inversion results by real-time or time-lapse inversion and, with the updated DFN parameters or hydraulic properties, the in-situ optimization and control of the relevant operation parameters.

CRedit authorship contribution statement

Lisa Maria Ringel: Conceptualization, Visualization, Writing – original draft. **Walter A. Illman:** Conceptualization, Writing – review & editing. **Peter Bayer:** Conceptualization, Writing – review & editing.

Declaration of competing interest

The authors declare that they have no known competing financial interests or personal relationships that could have appeared to influence the work reported in this paper.

Data availability

No data was used for the research described in the article.

Acknowledgments

We thank Zhibing Yang, an anonymous reviewer, and the Associate Editor for their valuable and constructive comments. The contributions by Lisa Maria Ringel and Peter Bayer were funded by the German Research Foundation (DFG), grant number BA-2850-5-1. Walter A. Illman acknowledges the support from the Discovery Grant from the Natural Sciences and Engineering Research Council of Canada (NSERC) which made this collaboration possible.

References

- Adler, P.M., Thovert, J.-F., Mourzenko, V.V., 2013. *Fractured Porous Media*. Oxford University Press, Oxford.
- Afshari Moein, M.J., Somogyvári, M., Valley, B., Jalali, M., Loew, S., Bayer, P., 2018. Fracture network characterization using stress-based tomography. *J. Geophys. Res. Solid Earth* 123 (11), 9324–9340. <https://doi.org/10.1029/2018JB016438>.
- Amann, F., Gischig, V., Evans, K., Doetsch, J., Jalali, R., Valley, B., Krietsch, H., Dutler, N., Villiger, L., Brixel, B., Klepikova, M., Kittilä, A., Madonna, C., Wiemer, S., Saar, M.O., Loew, S., Driesner, T., Maurer, H., Giardini, D., 2018. The seismo-hydrromechanical behavior during deep geothermal reservoir stimulations: open questions tackled in a decameter-scale in situ stimulation experiment. *Solid Earth* 9 (1), 115–137. <https://doi.org/10.5194/se-9-115-2018>.
- Armand, G., Leveau, F., Nussbaum, C., de La Vaissière, R., Noiret, A., Jaeggi, D., Landrein, P., Righini, C., 2014. Geometry and properties of the excavation-induced fractures/haute-marie URL Drifts. *Rock Mech Rock Eng* 47 (1), 21–41. <https://doi.org/10.1007/s00603-012-0339-6>.
- Aster, R.C., Borchers, B., Thurber, C.H., 2018. *Parameter Estimation and Inverse Problems*. Elsevier, Amsterdam, Netherlands, Kidlington, Oxford, England, Cambridge, Massachusetts.
- Barthélémy, J.-F., Guiton, M.L., Daniel, J.-M., 2009. Estimates of fracture density and uncertainties from well data. *Int. J. Rock Mech. Min. Sci.* 46 (3), 590–603. <https://doi.org/10.1016/j.ijrmms.2008.08.003>.
- Berkowitz, B., 2002. Characterizing flow and transport in fractured geological media: A review. *Adv. Water Resour.* 25 (8–12), 861–884. [https://doi.org/10.1016/S0309-1708\(02\)00042-8](https://doi.org/10.1016/S0309-1708(02)00042-8).
- Berre, I., Doster, F., Keilegavlen, E., 2019. Flow in fractured porous media: A review of conceptual models and discretization approaches. *Transp. Porous Media* 130, 215–236. <https://doi.org/10.1007/s11242-018-1171-6>.
- Blessent, D., Therrien, R., Lemieux, J.-M., 2011. Inverse modeling of hydraulic tests in fractured crystalline rock based on a transition probability geostatistical approach. *Water Resour. Res.* 47 (12), W12530. <https://doi.org/10.1029/2011WR011037>.
- Bour, O., Davy, P., 1997. Connectivity of random fault networks following a power law fault length distribution. *Water Resour. Res.* 33 (7), 1567–1583. <https://doi.org/10.1029/96WR00433>.
- Brauchler, R., Liedl, R., Dietrich, P., 2003. A travel time based hydraulic tomographic approach. *Water Resour. Res.* 39 (12), 1370. <https://doi.org/10.1029/2003wr002262>.
- Brauchler, R., Böhm, G., Leven, C., Dietrich, P., Sauter, M., 2013a. A laboratory study of tracer tomography. *Hydrol. J.* 21 (6), 1265–1274. <https://doi.org/10.1007/s10040-013-1006-z>.
- Brauchler, R., Hu, R., Hu, L., Jiménez, S., Bayer, P., Dietrich, P., Ptak, T., 2013b. Rapid field application of hydraulic tomography for resolving aquifer heterogeneity in unconsolidated sediments. *Water Resour. Res.* 49 (4), 2013–2024. <https://doi.org/10.1002/wrcr.20181>.
- Brixel, B., Klepikova, M., Jalali, M., Lei, Q., Roques, C., Krietsch, H., Loew, S., 2020a. Tracking fluid flow in shallow crustal fault zones: 1. insights from single-hole permeability estimates. *J. Geophys. Res.: Solid Earth* 125 (4), e2019JB018200. <https://doi.org/10.1029/2019JB018200>.
- Brixel, B., Roques, C., Krietsch, H., Klepikova, M., Jalali, M., Lei, Q., Loew, S., 2020b. Tracking fluid flow in shallow crustal fault zones: 2. Insights from cross-hole forced flow experiments in damage zones. *J. Geophys. Res.: Solid Earth* 125 (4), e2019JB019108. <https://doi.org/10.1029/2019JB019108>.
- Cardiff, M., Barrash, W., 2011. 3-D transient hydraulic tomography in unconfined aquifers with fast drainage response. *Water Resour. Res.* 47 (12), W12518. <https://doi.org/10.1029/2010wr010367>.
- Carrera, J., Alcolea, A., Medina, A., Hidalgo, J., Slooten, L.J., 2005. Inverse problem in hydrogeology. *Hydrogeol. J.* 13 (1), 206–222. <https://doi.org/10.1007/s10040-004-0404-7>.
- Chandra, S., Auken, E., Maurya, P.K., Ahmed, S., Verma, S.K., 2019. Large scale mapping of fractures and groundwater pathways in crystalline hardrock by AEM. *Sci Rep* 9 (1), 1–11. <https://doi.org/10.1038/s41598-018-36153-1>.
- Chen, G., Luo, X., Jiao, J.J., Jiang, C., 2023. Fracture network characterization with deep generative model based stochastic inversion. *Energy* 273, 127302. <https://doi.org/10.1016/j.energy.2023.127302>.
- Chuang, P.-Y., Chia, Y., Chiu, Y.-C., Teng, M.-H., Liou, S.Y.H., 2017. Mapping fracture flow paths with a nanoscale zero-valent iron tracer test and a flowmeter test. *Hydrol. J.* 26 (1), 321–331. <https://doi.org/10.1007/s10040-017-1651-8>.
- Cliffe, K., Holton, D., Houston, P., Jackson, C.B., Joyce, S., Milne, A., 2011. Conditioning discrete fracture network models of groundwater flow. *Int. J. Numer. Anal. Model.* 8 (4), 543–565.
- Cvetkovic, V., Cheng, H., 2011. Evaluation of single-well injection-withdrawal tests in Swedish crystalline rock using the Lagrangian travel time approach. *Water Resour. Res.* 47 (2), W02527. <https://doi.org/10.1029/2010WR009627>.
- Cvetkovic, V., Cheng, H., Widestrand, H., Byegård, J., Winberg, A., Andersson, P., 2007. Sorbing tracer experiments in a crystalline rock fracture at Äspö (Sweden): 2. Transport model and effective parameter estimation. *Water Resour. Res.* 43 (11), W11421. <https://doi.org/10.1029/2006WR005278>.
- Cvetkovic, V., Cheng, H., Byegård, J., Winberg, A., Tullborg, E.-L., Widestrand, H., 2010. Transport and retention from single to multiple fractures in crystalline rock at Äspö (Sweden): 1. Evaluation of tracer test results and sensitivity analysis. *Water Resour. Res.* 46 (5), W05505. <https://doi.org/10.1029/2009WR008013>.
- Day-Lewis, F.D., Slater, L.D., Robinson, J., Johnson, C.D., Terry, N., Werkema, D., 2017. An overview of geophysical technologies appropriate for characterization and monitoring at fractured-rock sites. *J. Environ. Manage.* 204, 709–720. <https://doi.org/10.1016/j.jenvman.2017.04.033>.
- de Dreuzy, J.-R., Méheust, Y., Pichot, G., 2012. Influence of fracture scale heterogeneity on the flow properties of three-dimensional discrete fracture networks (DFN). *J. Geophys. Res. Solid Earth* 117, B11207. <https://doi.org/10.1029/2012JB009461>.
- de La Bernardie, J., Bour, O., Le Borgne, T., Guihéneuf, N., Chatton, E., Labasque, T., Le Lay, H., Gerard, M.-F., 2018. Thermal attenuation and lag time in fractured rock: theory and field measurements from joint heat and solute tracer tests. *Water Resour. Res.* 54 (12), 10053–10075. <https://doi.org/10.1029/2018WR023199>.
- de La Vaissière, R., Armand, G., Talandier, J., 2015. Gas and water flow in an excavation-induced fracture network around an underground drift: A case study for a radioactive waste repository in clay rock. *J. Hydrol.* 521, 141–156. <https://doi.org/10.1016/j.jhydrol.2014.11.067>.
- Dodangeh, A., Rajabi, M.M., Fahs, M., 2023. Combining harmonic pumping with a tracer test for fractured aquifer characterization. *Hydrogeol. J.* 31 (2), 371–385. <https://doi.org/10.1007/s10040-023-02595-9>.
- Doetsch, J., Linde, N., Vogt, T., Binley, A., Green, A.G., 2012. Imaging and quantifying salt-tracer transport in a riparian groundwater system by means of 3D ERT

- monitoring. *Geophysics* 77 (5), B207–B218. <https://doi.org/10.1190/geo2012-0046.1>.
- Dong, Y., Fu, Y., Yeh, T.-C.-J., Wang, Y.-L., Zha, Y., Wang, L., Hao, Y., 2019. Equivalence of discrete fracture network and porous media models by hydraulic tomography. *Water Resour. Res.* 55 (4), 3234–3247. <https://doi.org/10.1029/2018wr024290>.
- Dorn, C., Linde, N., Le Borgne, T., Bour, O., de Dreuzy, J.-R., 2013. Conditioning of stochastic 3-D fracture networks to hydrological and geophysical data. *Adv. Water Resour.* 62, 79–89. <https://doi.org/10.1016/j.advwatres.2013.10.005>.
- Fischer, P., Jardani, A., Lecoq, N., 2017a. A cellular automata-based deterministic inversion algorithm for the characterization of linear structural heterogeneities. *Water Resour. Res.* 53 (3), 2016–2034. <https://doi.org/10.1002/2016WR019572>.
- Fischer, P., Jardani, A., Wang, X., Jourde, H., Lecoq, N., 2017b. Identifying flow networks in a karstified aquifer by application of the cellular automata-based deterministic inversion method (Lez Aquifer, France). *Water Resour. Res.* 53 (12), 10508–10522. <https://doi.org/10.1002/2017wr020921>.
- Fischer, P., Jardani, A., Cardiff, M., Lecoq, N., Jourde, H., 2018a. Hydraulic analysis of harmonic pumping tests in frequency and time domains for identifying the conduits networks in a karstic aquifer. *J. Hydrol.* 559, 1039–1053. <https://doi.org/10.1016/j.jhydrol.2018.03.010>.
- Fischer, P., Jardani, A., Jourde, H., Cardiff, M., Wang, X., Chedeville, S., Lecoq, N., 2018b. Harmonic pumping tomography applied to image the hydraulic properties and interpret the connectivity of a karstic and fractured aquifer (Lez aquifer, France). *Adv. Water Resour.* 119, 227–244. <https://doi.org/10.1016/j.advwatres.2018.07.002>.
- Fischer, P., Jardani, A., Lecoq, N., 2018c. Hydraulic tomography of discrete networks of conduits and fractures in a karstic aquifer by using a deterministic inversion algorithm. *Adv. Water Resour.* 112, 83–94. <https://doi.org/10.1016/j.advwatres.2017.11.029>.
- Fischer, P., Jardani, A., Jourde, H., 2020. Hydraulic tomography in coupled discrete-continuum concept to image hydraulic properties of a fractured and karstified aquifer (Lez aquifer, France). *Adv. Water Resour.* 137, 103523. <https://doi.org/10.1016/j.advwatres.2020.103523>.
- Follin, S., Hartley, L., Rhén, I., Jackson, P., Joyce, S., Roberts, D., Swift, B., 2014. A methodology to constrain the parameters of a hydrogeological discrete fracture network model for sparsely fractured crystalline rock, exemplified by data from the proposed high-level nuclear waste repository site at Forsmark, Sweden. *Hydrogeol. J.* 22 (2), 313–331. <https://doi.org/10.1007/s10040-013-1080-2>.
- Frampton, A., Cvetkovic, V., 2010. Inference of field-scale fracture transmissivities in crystalline rock using flow log measurements. *Water Resour. Res.* 46 (11), W11502. <https://doi.org/10.1029/2009WR008367>.
- Giertzuch, P.-L., Doetsch, J., Shakas, A., Jalali, M., Brixel, B., Maurer, H., 2021a. Four-dimensional tracer flow reconstruction in fractured rock through borehole ground-penetrating radar (GPR) monitoring. *Solid Earth* 12 (7), 1497–1513. <https://doi.org/10.5194/se-12-1497-2021>.
- Giertzuch, P.-L., Shakas, A., Doetsch, J., Brixel, B., Jalali, M., Maurer, H., 2021b. Computing localized breakthrough curves and velocities of saline tracer from ground penetrating radar monitoring experiments in fractured rock. *Energies* 14 (10), 2949. <https://doi.org/10.3390/en14102949>.
- Guo, Q., Zhao, Y., Lu, C., Luo, J., 2023. High-dimensional inverse modeling of hydraulic tomography by physics informed neural network (HT-PINN). *J. Hydrol.* 616, 128828. <https://doi.org/10.1016/j.jhydrol.2022.128828>.
- Guzman, A.G., Geddis, A.M., Henrich, M.J., Lohrstorfer, C.F., Neuman, S.P., 1996. Summary of Air Permeability Data From Single-Hole Injection Tests in Unsaturated Fractured Tuffs at the Apache Leap Research Site: Results of Steady-State Test Interpretation. U.S. Nuclear Regulatory Research, Washington, D.C.
- Hadgu, T., Karra, S., Kalinina, E., Makedonska, N., Hyman, J.D., Klise, K., Viswanathan, H.S., Wang, Y., 2017. A comparative study of discrete fracture network and equivalent continuum models for simulating flow and transport in the far field of a hypothetical nuclear waste repository in crystalline host rock. *J. Hydrol.* 553, 59–70. <https://doi.org/10.1016/j.jhydrol.2017.07.046>.
- Hao, Y., Yeh, T.-C.-J., Xiang, J., Illman, W.A., Ando, K., Hsu, K.-C., Lee, C.-H., 2008. Hydraulic tomography for detecting fracture zone connectivity. *Ground Water* 46 (2), 183–192. <https://doi.org/10.1111/j.1745-6584.2007.00388.x>.
- Hermans, T., Wildemeersch, S., Jamin, P., Orban, P., Brouyère, S., Dassargues, A., Nguyen, F., 2015. Quantitative temperature monitoring of a heat tracing experiment using cross-borehole ERT. *Geothermics* 53, 14–26. <https://doi.org/10.1016/j.geothermics.2014.03.013>.
- Hsieh, P.A., Neuman, S.P., Simpson, E.S., 1983. Pressure Testing of Fractured Rocks - A Methodology Employing Three-Dimensional Cross-Hole Tests. U.S. Nuclear Regulatory Commission, Washington, D.C.
- Hsieh, P.A., Neuman, S.P., Stiles, G.K., Simpson, E.S., 1985. Field determination of the three-dimensional hydraulic conductivity tensor of anisotropic media: 2. Methodology and application to fractured rocks. *Water Resour. Res.* 21 (11), 1667–1676. <https://doi.org/10.1029/WR021i11p01667>.
- Hyman, J.D., Dentz, M., Hagberg, A., Kang, P.K., 2019. Linking structural and transport properties in three-dimensional fracture networks. *J. Geophys. Res. Solid Earth* 124 (2), 1185–1204. <https://doi.org/10.1029/2018jb016553>.
- Illman, W.A., 2014. Hydraulic tomography offers improved imaging of heterogeneity in fractured rocks. *Groundwater* 52 (5), 659–684. <https://doi.org/10.1111/gwat.12119>.
- Illman, W.A., Neuman, S.P., 2000. Type-curve interpretation of multirate single-hole pneumatic injection tests in unsaturated fractured rock. *Ground Water* 38 (6), 899–911. <https://doi.org/10.1111/j.1745-6584.2000.tb00690.x>.
- Illman, W.A., Neuman, S.P., 2001. Type curve interpretation of a cross-hole pneumatic injection test in unsaturated fractured tuff. *Water Resour. Res.* 37 (3), 583–603. <https://doi.org/10.1029/2000WR900273>.
- Illman, W.A., Liu, X., Takeuchi, S., Jim Yeh, T.-C., Ando, K., Saegusa, H., 2009. Hydraulic tomography in fractured granite: Mizunami Underground Research site, Japan. *Water Resour. Res.* 45 (1), W01406. <https://doi.org/10.1029/2007WR006715>.
- Illman, W.A., Berg, S.J., Liu, X., Massi, A., 2010. Hydraulic/partitioning tracer tomography for DNAPL source zone characterization: small-scale sandbox experiments. *Environ. Sci. Tech.* 44 (22), 8609–8614. <https://doi.org/10.1021/es101654j>.
- Ishibashi, M., Yoshida, H., Sasao, E., Yuguchi, T., 2016. Long term behavior of hydrogeological structures associated with faulting: An example from the deep crystalline rock in the Mizunami URL, Central Japan. *Eng. Geol.* 208, 114–127. <https://doi.org/10.1016/j.enggeo.2016.04.026>.
- Jalali, M., Brauchler, R., Somogyvári, M., La Vaissière, R. de, 2023. High-resolution characterization of excavation-induced fracture network using continuous and discrete inversion schemes. *Water Resour. Res.*, 59 (10), e2022WR033962. <https://doi.org/10.1029/2022WR033962>.
- Jalali, M., Klepikova, M., Doetsch, J., Krietsch, H., Brixel, B., Dutler, N., Gischig, V., Amann, F., 2018. A multi-scale approach to identify and characterize preferential flow paths in a fractured crystalline rock. *Proceedings of the 52nd u.s. Rock Mechanics/Geomechanics Symposium. American Rock Mechanics Association.*
- Jardani, A., Revil, A., Dupont, J.P., 2013. Stochastic joint inversion of hydrogeophysical data for salt tracer test monitoring and hydraulic conductivity imaging. *Adv. Water Resour.* 52, 62–77. <https://doi.org/10.1016/j.advwatres.2012.08.005>.
- Jiang, Z., Ringel, L.M., Bayer, P., Xu, T., 2023. Fracture network characterization in reservoirs by joint inversion of microseismicity and thermal breakthrough data: method development and verification. *Water Resour. Res.*, 59 (9), e2022WR034339. <https://doi.org/10.1029/2022WR034339>.
- Kang, P.K., Le Borgne, T., Dentz, M., Bour, O., Juanes, R., 2015. Impact of velocity correlation and distribution on transport in fractured media: Field evidence and theoretical model. *Water Resour. Res.* 51 (2), 940–959. <https://doi.org/10.1002/2014WR015799>.
- Kitanidis, P.K., 1995. Quasi-linear geostatistical theory for inverting. *Water Resour. Res.* 31 (10), 2411–2419. <https://doi.org/10.1029/95WR01945>.
- Kittilä, A., Jalali, M., Evans, K.F., Willmann, M., Saar, M.O., Kong, X.-Z., 2019. Field comparison of DNA-labeled nanoparticle and solute tracer transport in a fractured crystalline rock. *Water Resour. Res.* 55 (8), 6577–6595. <https://doi.org/10.1029/2019WR025021>.
- Kittilä, A., Jalali, M.R., Somogyvári, M., Evans, K.F., Saar, M.O., Kong, X.-Z., 2020. Characterization of the effects of hydraulic stimulation with tracer-based temporal moment analysis and tomographic inversion. *Geothermics* 86, 101820. <https://doi.org/10.1016/j.geothermics.2020.101820>.
- Klepikova, M., Brixel, B., Jalali, M., 2020. Transient hydraulic tomography approach to characterize main flowpaths and their connectivity in fractured media. *Adv. Water Resour.* 136, 103500. <https://doi.org/10.1016/j.advwatres.2019.103500>.
- Klepikova, M.V., Le Borgne, T., Bour, O., de Dreuzy, J.-R., 2013. Inverse modeling of flow tomography experiments in fractured media. *Water Resour. Res.* 49 (11), 7255–7265. <https://doi.org/10.1002/2013WR013722>.
- Klepikova, M.V., Le Borgne, T., Bour, O., Gallagher, K., Hochreutener, R., Lavenant, N., 2014. Passive temperature tomography experiments to characterize transmissivity and connectivity of preferential flow paths in fractured media. *J. Hydrol.* 512, 549–562. <https://doi.org/10.1016/j.jhydrol.2014.03.018>.
- Krietsch, H., Doetsch, J., Dutler, N., Jalali, M., Gischig, V., Loew, S., Amann, F., 2018. Comprehensive geological dataset describing a crystalline rock mass for hydraulic stimulation experiments. *Sci. Data* 5, 180269. <https://doi.org/10.1038/sdata.2018.269>.
- Le Borgne, T., Paillet, F., Bour, O., Caudal, J.-P., 2006. Cross-borehole flowmeter tests for transient heads in heterogeneous aquifers. *Groundwater* 44 (3), 444–452. <https://doi.org/10.1111/j.1745-6584.2005.00150.x>.
- Le Goc, R., de Dreuzy, J.-R., Davy, P., 2010. An inverse problem methodology to identify flow channels in fractured media using synthetic steady-state head and geometrical data. *Adv. Water Resour.* 33 (7), 782–800. <https://doi.org/10.1016/j.advwatres.2010.04.011>.
- Lei, Q., Latham, J.-P., Tsang, C.-F., 2017. The use of discrete fracture networks for modelling coupled geomechanical and hydrological behaviour of fractured rocks. *Comput. Geotech.* 85, 151–176. <https://doi.org/10.1016/j.compgeo.2016.12.024>.
- Li, S., Wang, X., Xu, Z., Mao, D., Pan, D., 2021. Numerical investigation of hydraulic tomography for mapping karst conduits and its connectivity. *Eng. Geol.* 281, 105967. <https://doi.org/10.1016/j.enggeo.2020.105967>.
- Li, L., Zhang, Q., Zhou, Z., Cui, Y., Shao, J., Zhao, Y., 2022. Groundwater circulation patterns in bedrock aquifers from a pre-selected area of high-level radioactive waste repository based on two-dimensional numerical simulation. *J. Hydrol.* 610, 127849. <https://doi.org/10.1016/j.jhydrol.2022.127849>.
- Liu, Q., Hu, R., Hu, L., Xing, Y., Qiu, P., Yang, H., Fischer, S., Ptak, T., 2022. Investigation of hydraulic properties in fractured aquifers using cross-well travel-time based thermal tracer tomography: Numerical and field experiments. *J. Hydrol.* 609, 127751. <https://doi.org/10.1016/j.jhydrol.2022.127751>.
- Liu, Q., Hu, L., Hu, R., Brauchler, R., Xing, Y., Qi, J., Ptak, T., 2023. Characterization of aquifer heterogeneity by tomographic slug test responses considering wellbore effects. *J. Hydrol.* 130472. <https://doi.org/10.1016/j.jhydrol.2023.130472>.
- Luo, N., Zhao, Z., Illman, W.A., Zha, Y., Mok, C.M.W., Yeh, T.-C.-J., 2023. Three-dimensional steady-state hydraulic tomography analysis with integration of cross-hole flowmeter data at a highly heterogeneous site. *Water Resour. Res.*, 59 (6), e2022WR034034. <https://doi.org/10.1029/2022WR034034>.
- Ma, X., Zhang, K., Yao, C., Zhang, L., Wang, J., Yang, Y., Yao, J., 2020. Multiscale-network structure inversion of fractured media based on a hierarchical-parameterization and data-driven evolutionary-optimization method. *SPE J.* 25 (5), 2729–2748. <https://doi.org/10.2118/201237-pa>.

- Ma, X., Hertrich, M., Amann, F., Bröker, K., Gholizadeh Doonechaly, N., Gischig, V., Hochreutener, R., Kästli, P., Krietsch, H., Marti, M., Nägeli, B., Nejati, M., Obermann, A., Plenkers, K., Rinaldi, A.P., Shakas, A., Villiger, L., Wenning, Q., Zappone, A., Bethmann, F., Castilla, R., Seberto, F., Meier, P., Driesner, T., Loew, S., Maurer, H., Saar, M.O., Wiemer, S., Giardini, D., 2022. Multi-disciplinary characterizations of the BedrettoLab – a new underground geoscience research facility. *Solid Earth* 13 (2), 301–322. <https://doi.org/10.5194/se-13-301-2022>.
- Mao, D., Liu, Z., Wang, W., Li, S., Gao, Y., Xu, Z., Zhang, C., 2018. An application of hydraulic tomography to a deep coal mine: combining traditional pumping tests with water inrush incidents. *J. Hydrol.* 567, 1–11. <https://doi.org/10.1016/j.jhydrol.2018.09.058>.
- Massiot, C., Townend, J., Nicol, A., McNamara, D.D., 2017. Statistical methods of fracture characterization using acoustic borehole televiewer log interpretation. *J. Geophys. Res. Solid Earth* 122 (8), 6836–6852. <https://doi.org/10.1002/2017JB014115>.
- Meier, P.M., Medina, A., Carrera, J., 2001. Geostatistical inversion of cross-hole pumping tests for identifying preferential flow channels within a shear zone. *Ground Water* 39 (1), 10–17. <https://doi.org/10.1111/j.1745-6584.2001.tb00346.x>.
- Mohammadi, Z., Illman, W.A., 2019. Detection of karst conduit patterns via hydraulic tomography: A synthetic inverse modeling study. *J. Hydrol.* 572, 131–147. <https://doi.org/10.1016/j.jhydrol.2019.02.044>.
- Mourzenko, V.V., Thovert, J.-F., Adler, P.M., 2018. Conductivity and transmissivity of a single fracture. *Transp Porous Med* 123 (2), 235–256. <https://doi.org/10.1007/s11242-018-1037-y>.
- Neuman, S.P., 1987. Stochastic continuum representation of fractured rock permeability as an alternative to the REV and fracture network concepts. In: *Proceedings of the 28th u.s. Symposium on Rock Mechanics*, pp. 533–561.
- Neuman, S.P., 2005. Trends, prospects and challenges in quantifying flow and transport through fractured rocks. *Hydrol. J.* 13 (1), 124–147. <https://doi.org/10.1007/s10040-004-0397-2>.
- Neuman, S.P., Walter, G.R., Bentley, H.W., Ward, J.J., Gonzalez, D.D., 1984. Determination of horizontal aquifer anisotropy with three wells. *Groundwater* 22 (1), 66–72. <https://doi.org/10.1111/j.1745-6584.1984.tb01477.x>.
- Ni, C.-F., Yeh, T.-C.-J., 2008. Stochastic inversion of pneumatic cross-hole tests and barometric pressure fluctuations in heterogeneous unsaturated formations. *Adv. Water Resour.* 31 (12), 1708–1718. <https://doi.org/10.1016/j.advwatres.2008.08.007>.
- Paillet, F.L., 1995. Practical hydraulic tomography in heterogeneous fractured aquifers, symposium on the application of geophysics to engineering and environmental problems 1995. *Environ. Eng. Geophys. Soc.* 559–569.
- Paillet, F.L., Morin, R.H., 1997. Hydraulic tomography in fractured bedrock aquifers using high-resolution borehole flowmeter measurements. *Geol. Soc., London, Eng. Geol. Special Publications* 12 (1), 267–272. <https://doi.org/10.1144/GSL.ENG.1997.012.01.23>.
- Panzeri, M., Riva, M., Guadagnini, A., Neuman, S.P., 2013. Data assimilation and parameter estimation via ensemble Kalman filter coupled with stochastic moment equations of transient groundwater flow. *Water Resour. Res.* 49 (3), 1334–1344. <https://doi.org/10.1002/wrcr.20113>.
- Park, Y.-J., Sudicky, E.A., McLaren, R.G., Sykes, J.F., 2004. Analysis of hydraulic and tracer response tests within moderately fractured rock based on a transition probability geostatistical approach. *Water Resour. Res.* 40 (12), W12404. <https://doi.org/10.1029/2004WR003188>.
- Pavičić, I., Galić, I., Kucelj, M., Dragičević, I., 2021. Fracture system and rock-mass characterization by borehole camera surveying: application in dimension stone investigations in geologically complex structures. *Appl. Sci.* 11 (2), 764. <https://doi.org/10.3390/app11020764>.
- Poduri, S., Kambhammettu, B., Gorugantula, S., 2021. A new randomized binary prior model for hydraulic tomography in fractured aquifers. *Groundwater* 59 (4), 537–548. <https://doi.org/10.1111/gwat.13074>.
- Qiu, H., Hu, R., Luo, N., Illman, W.A., Hou, X., 2023. Comparison of travel-time and geostatistical inversion approaches for hydraulic tomography: Synthetic modeling study on data density and well configuration issues. *J. Hydrol.* 618, 129247. <https://doi.org/10.1016/j.jhydrol.2023.129247>.
- Redolozo, F., Li, L., Davis, A., 2023. Stochastic inversion of discrete fracture networks using genetic algorithms. *Adv. Water Resour.* 178, 104477. <https://doi.org/10.1016/j.advwatres.2023.104477>.
- Ren, S., Zhang, Y., Jim Yeh, T.-C., Wang, Y., Carr, B.J., 2021. Multiscale hydraulic conductivity characterization in a fractured granitic aquifer: the evaluation of scale effect. *Water Resour. Res.*, 57 (9), e2020WR028482. <https://doi.org/10.1029/2020WR028482>.
- Ren, S., Gragg, S., Zhang, Y., Carr, B.J., Yao, G., 2018. Borehole characterization of hydraulic properties and groundwater flow in a crystalline fractured aquifer of a headwater mountain watershed, Laramie Range, Wyoming. *J. Hydrol.* 561, 780–795. <https://doi.org/10.1016/j.jhydrol.2018.04.048>.
- Ringel, L.M., Jalali, M., Bayer, P., 2021. Stochastic inversion of three-dimensional discrete fracture network structure with hydraulic tomography. *Water Resour. Res.*, 57 (12), e2021WR030401. <https://doi.org/10.1029/2021WR030401>.
- Ringel, L.M., Somogyvári, M., Jalali, M., Bayer, P., 2019. Comparison of hydraulic and tracer tomography for discrete fracture network inversion. *Geosciences* 9 (6), 274. <https://doi.org/10.3390/geosciences9060274>.
- Ringel, L.M., Jalali, M., Bayer, P., 2022. Characterization of the highly fractured zone at the Grimsel Test Site based on hydraulic tomography. *Hydrol. Earth Syst. Sci.* 26 (24), 6443–6455. <https://doi.org/10.5194/hess-26-6443-2022>.
- Sharmeen, R., Illman, W.A., Berg, S.J., Yeh, T.-C.-J., Park, Y.-J., Sudicky, E.A., Ando, K., 2012. Transient hydraulic tomography in a fractured dolostone: Laboratory rock block experiments. *Water Resour. Res.* 48 (10), W10532. <https://doi.org/10.1029/2012WR012216>.
- Somogyvári, M., Bayer, P., Brauchler, R., 2016. Travel-time-based thermal tracer tomography. *Hydrol. Earth Syst. Sci.* 20 (5), 1885–1901. <https://doi.org/10.5194/hess-20-1885-2016>.
- Somogyvári, M., Jalali, M., Parras, S.J., Bayer, P., 2017. Synthetic fracture network characterization with transdimensional inversion. *Water Resour. Res.* 53 (6), 5104–5123. <https://doi.org/10.1002/2016WR020293>.
- Somogyvári, M., Kühn, M., Reich, S., 2019. Reservoir-scale transdimensional fracture network inversion. *Adv. Geosci.* 49, 207–214. <https://doi.org/10.5194/adgeo-49-207-2019>.
- Spencer, S.A., Anderson, A.E., Silins, U., Collins, A.L., 2021. Hillslope and groundwater contributions to streamflow in a Rocky Mountain watershed underlain by glacial till and fractured sedimentary bedrock. *Hydrol. Earth Syst. Sci.* 25 (1), 237–255. <https://doi.org/10.5194/hess-25-237-2021>.
- Tiedeman, C.R., Barrash, W., 2020. Hydraulic tomography: 3D hydraulic conductivity, fracture network, and connectivity in mudstone. *Groundwater* 58 (2), 238–257. <https://doi.org/10.1111/gwat.12915>.
- Tiedeman, C.R., Lacombe, P.J., Goode, D.J., 2010. Multiple well-shutdown tests and site-scale flow simulation in fractured rocks. *Groundwater* 48 (3), 401–415. <https://doi.org/10.1111/j.1745-6584.2009.00651.x>.
- Trabucchi, M., Fernández-García, D., Carrera, J., 2022. The worth of stochastic inversion for identifying connectivity by means of a long-lasting large-scale hydraulic test: the salar de atacama case study. *Water Resour. Res.*, 58 (6), e2021WR030676. <https://doi.org/10.1029/2021WR030676>.
- Tsang, Y.W., Tsang, C.F., Hale, F.V., Dverstorp, B., 1996. Tracer transport in a stochastic continuum model of fractured media. *Water Resour. Res.* 32 (10), 3077–3092. <https://doi.org/10.1029/96WR01397>.
- Vasco, D.W., Datta-Gupta, A., 1999. Asymptotic solutions for solute transport: A formalism for tracer tomography. *Water Resour. Res.* 35 (1), 1–16. <https://doi.org/10.1029/98WR02742>.
- Vesselinov, V.V., Neuman, S.P., Illman, W.A., 2001a. Three-dimensional numerical inversion of pneumatic cross-hole tests in unsaturated fractured tuff: 1. Methodology and borehole effects. *Water Resour. Res.* 37 (12), 3001–3017. <https://doi.org/10.1029/2000WR000133>.
- Vesselinov, V.V., Neuman, S.P., Illman, W.A., 2001b. Three-dimensional numerical inversion of pneumatic cross-hole tests in unsaturated fractured tuff: 2. Equivalent parameters, high-resolution stochastic imaging and scale effects. *Water Resour. Res.* 37 (12), 3019–3041. <https://doi.org/10.1029/2000WR000135>.
- Vickers, B.C., Neuman, S.P., Sully, M.J., Evans, D.D., 1992. Reconstruction and geostatistical analysis of multiscale fracture apertures in a large block of welded tuff. *Geophys. Res. Lett.* 19 (10), 1029–1032. <https://doi.org/10.1029/92GL00560>.
- Viswanathan, H.S., Ajo-Franklin, J., Birkholzer, J.T., Carey, J.W., Guglielmi, Y., Hyman, J.D., Karra, S., Pyrak-Nolte, L.J., Rajaram, H., Srinivasan, G., Tartakovsky, D.M., 2022. From fluid flow to coupled processes in fractured rock: recent advances and new frontiers. *Rev. Geophys.*, 60 (1), e2021RG000744. <https://doi.org/10.1029/2021RG000744>.
- Vogler, D., Walsh, S.D.C., Bayer, P., Amann, F., 2017. Comparison of surface properties in natural and artificially generated fractures in a crystalline rock. *Rock Mech Rock Eng* 50 (11), 2891–2909. <https://doi.org/10.1007/s00603-017-1281-4>.
- Vogler, D., Settgaß, R.R., Annavarapu, C., Madonna, C., Bayer, P., Amann, F., 2018. Experiments and simulations of fully hydro-mechanically coupled response of rough fractures exposed to high-pressure fluid injection. *J. Geophys. Res. Solid Earth* 123 (2), 1186–1200. <https://doi.org/10.1002/2017JB015057>.
- Vu, M.T., Jardani, A., 2022. Mapping discrete fracture networks using inversion of hydraulic tomography data with convolutional neural network: SegNet-Fracture. *J. Hydrol.* 609, 127752. <https://doi.org/10.1016/j.jhydrol.2022.127752>.
- Vu, M.T., Jardani, A., 2023. Multitasking neural network to jointly map discrete fracture structures and matrix transmissivity by inverting hydraulic data acquired in 2D fractured aquifers. *XNET-Fracture*. *Adv. Water Resour.* 177, 104463. <https://doi.org/10.1016/j.advwatres.2023.104463>.
- Wang, X., Jardani, A., Jourde, H., Lonergan, L., Cosgrove, J., Gosselin, O., Massonnat, G., 2016. Characterisation of the transmissivity field of a fractured and karstic aquifer, Southern France. *Adv. Water Resour.* 87, 106–121. <https://doi.org/10.1016/j.advwatres.2015.10.014>.
- Wang, X., Jardani, A., Jourde, H., 2017. A hybrid inverse method for hydraulic tomography in fractured and karstic media. *J. Hydrol.* 551, 29–46. <https://doi.org/10.1016/j.jhydrol.2017.05.051>.
- Wang, X., Xu, Z., Hu, J., 2023. A new attempt for the detection of potential water-bearing structures in tunnels via hydraulic tomography: The first numerical investigation. *Tunn. Undergr. Space Technol.* 135, 105034. <https://doi.org/10.1016/j.tust.2023.105034>.
- Wang, W., Zhao, W., Qian, J., Ma, L., Wang, D., Hou, X., 2021. Potential of hydraulic tomography in exploring the preferential flowpaths of water inrush in coal mine areas. *J. Hydrol.* 602, 126830. <https://doi.org/10.1016/j.jhydrol.2021.126830>.
- White, J.T., 2018. A model-independent iterative ensemble smoother for efficient history-matching and uncertainty quantification in very high dimensions. *Environ. Model. Softw.* 109, 191–201. <https://doi.org/10.1016/j.envsoft.2018.06.009>.
- Wilske, C., Suckow, A., Mallast, U., Meier, C., Merchel, S., Merkel, B., Pavetich, S., Rödig, T., Rugel, G., Sachse, A., Weise, S.M., Siebert, C., 2020. A multi-environmental tracer study to determine groundwater residence times and recharge in a structurally complex multi-aquifer system. *Hydrol. Earth Syst. Sci.* 24 (1), 249–267. <https://doi.org/10.5194/hess-24-249-2020>.
- Witherspoon, P.A., Wang, J.S.-Y., Iwai, K., Gale, J.E., 1980. Validity of Cubic Law for fluid flow in a deformable rock fracture. *Water Resour. Res.* 16 (6), 1016–1024. <https://doi.org/10.1029/WR016i06p1016>.
- Xiang, J., Yeh, T.-C.-J., Lee, C.-H., Hsu, K.-C., Wen, J.-C., 2009. A simultaneous successive linear estimator and a guide for hydraulic tomography analysis. *Water Resour. Res.* 45 (2) <https://doi.org/10.1029/2008WR007180>.

- Yang, H., Hu, R., Qiu, P., Liu, Q., Xing, Y., Tao, R., Ptak, T., 2020. Application of wavelet de-noising for travel-time based hydraulic tomography. *Water* 12 (6), 1533. <https://doi.org/10.3390/w12061533>.
- Yeh, T.-C.-J., Liu, S., 2000. Hydraulic tomography: development of a new aquifer test method. *Water Resour. Res.* 36 (8), 2095–2105. <https://doi.org/10.1029/2000WR900114>.
- Yeh, T.-C.-J., Mao, D., Zha, Y., Wen, J.-C., Wan, L., Hsu, K.-C., Lee, C.-H., 2015. Uniqueness, scale, and resolution issues in groundwater model parameter identification. *Water Sci. Eng.* 8 (3), 175–194. <https://doi.org/10.1016/j.wse.2015.08.002>.
- Yeh, T.-C.-J., Zhu, J., 2007. Hydraulic/partitioning tracer tomography for characterization of dense nonaqueous phase liquid source zones. *Water Resour. Res.* 43 (6), W06435. <https://doi.org/10.1029/2006WR004877>.
- Yeh, T.-C.-J., Jin, M., Hanna, S., 1996. An iterative stochastic inverse method: conditional effective transmissivity and hydraulic head fields. *Water Resour. Res.* 32 (1), 85–92. <https://doi.org/10.1029/95WR02869>.
- Yin, T., Chen, Q., 2020. Simulation-based investigation on the accuracy of discrete fracture network (DFN) representation. *Comput. Geotech.* 121, 103487. <https://doi.org/10.1016/j.compgeo.2020.103487>.
- Zha, Y., Yeh, T.-C.-J., Illman, W.A., Tanaka, T., Bruines, P., Onoe, H., Saegusa, H., 2015. What does hydraulic tomography tell us about fractured geological media? A field study and synthetic experiments. *J. Hydrol.* 531, 17–30. <https://doi.org/10.1016/j.jhydrol.2015.06.013>.
- Zha, Y., Yeh, T.-C.-J., Illman, W.A., Tanaka, T., Bruines, P., Onoe, H., Saegusa, H., Mao, D., Takeuchi, S., Wen, J.-C., 2016. An application of hydraulic tomography to a large-scale fractured granite site, Mizunami, Japan. *Ground Water* 54 (6), 793–804. <https://doi.org/10.1111/gwat.12421>.
- Zha, Y., Yeh, T.-C.-J., Illman, W.A., Onoe, H., Mok, C.M.W., Wen, J.-C., Huang, S.-Y., Wang, W., 2017. Incorporating geologic information into hydraulic tomography: A general framework based on geostatistical approach. *Water Resour. Res.* 53 (4), 2850–2876. <https://doi.org/10.1002/2016WR019185>.
- Zhao, H., Luo, N., Illman, W.A., 2021. The importance of fracture geometry and matrix data on transient hydraulic tomography in fractured rocks: Analyses of synthetic and laboratory rock block experiments. *J. Hydrol.* 601, 126700. <https://doi.org/10.1016/j.jhydrol.2021.126700>.
- Zhu, J., Yeh, T.-C.-J., 2005. Characterization of aquifer heterogeneity using transient hydraulic tomography. *Water Resour. Res.* 41 (7), W07028. <https://doi.org/10.1029/2004WR003790>.
- Zimmerman, R.W., Bodvarsson, G.S., 1996. Hydraulic conductivity of rock fractures. *Transp Porous Med* 23 (1), 1–30. <https://doi.org/10.1007/BF00145263>.